

# Local interactions and the role of the 6-120 disulfide bond in $\alpha$ -lactalbumin: implications for formation of the molten globule state

Daniel F. Moriarty<sup>a</sup>, Stephen J. Demarest<sup>a</sup>, James Robblee<sup>b</sup>, Robert Fairman<sup>b</sup>,  
Daniel P. Raleigh<sup>a,c,\*</sup>

<sup>a</sup> Department of Chemistry, State University of New York at Stony Brook, Stony Brook, NY 11794-3400, USA

<sup>b</sup> Department of Molecular, Cellular and Developmental Biology, Haverford College, Haverford, PA 19041, USA

<sup>c</sup> Graduate Program in Biophysics and Graduate Program in Molecular and Cellular Biology, State University of New York, Stony Brook, NY 11794, USA

Received 9 August 1999; accepted 28 September 1999

## Abstract

Molten globule states are partially folded states of proteins which are compact and contain a high degree of secondary structure but which lack many of the fixed tertiary interactions associated with the native state. A set of peptides has been prepared in order to probe the role of local interactions in the vicinity of the Cys<sup>6</sup>-Cys<sup>120</sup> disulfide bond in stabilizing the molten globule state of human  $\alpha$ -lactalbumin. Peptides derived from the N-terminal and C-terminal regions of human  $\alpha$ -lactalbumin have been analyzed using nuclear magnetic resonance, circular dichroism, fluorescence spectroscopy and sedimentation equilibrium experiments. A peptide corresponding to the first helical region in the native protein, residues 1–13, is only slightly helical in isolation. Extending the peptide to include residues 14–18 results in a modest increase in helicity. A peptide derived from the C-terminal 12 residues, residues 112–123, is predominantly unstructured. Crosslinking the N- and C-terminal peptides by the native disulfide bond results in almost no increase in structure and there is no evidence for any significant cooperative structure formation over the range of pH 2.2–11.7. These results demonstrate that there is very little enhancement of local structure due to the formation of the Cys<sup>6</sup>-Cys<sup>120</sup> disulfide bond. This is in striking contrast to peptides derived from the region of the Cys<sup>28</sup>-Cys<sup>111</sup> disulfide. © 2000 Elsevier Science B.V. All rights reserved.

**Keywords:** Molten globule;  $\alpha$ -Lactalbumin; Protein folding; Peptide model; Protein structure

## 1. Introduction

A growing number of proteins have been shown to

Abbreviations:  $\alpha$ -LA,  $\alpha$ -lactalbumin; ANS, 1-anilinonaphthalene-8-sulfonate; CD, circular dichroism; Cys, cysteine; DMF, *N,N*-dimethylformamide; Fmoc, 9-fluorenylmethyloxycarbonyl; HCl, hydrochloric acid; HPLC, high pressure liquid chromatography; MALDI, matrix-assisted laser desorption ionization; SA, 3,5-dimethoxy-4-hydroxy-cinnamic acid

\* Corresponding author. Fax: +1 (516) 632-7960;  
E-mail: draleigh@cmail.sunysb.edu

form stable partially folded states under mildly denaturing conditions. These states, known as molten globules, generally contain a high level of secondary structure and are compact, but have few specific tertiary contacts and are much less rigid than the native state [1–4]. In many cases, the equilibrium molten globule state is thought to provide an excellent mimic of partially folded structures populated during the folding process. Consequently, there has been a great deal of interest in characterizing the structure and the interactions which stabilize partially folded states.

$\alpha$ -Lactalbumin ( $\alpha$ -LA) has been shown to form a molten globule [5–7] that can be stabilized under a range of conditions including low pH [8,9]. This equilibrium intermediate is believed to closely resemble the kinetic intermediate that is transiently populated during the folding of  $\alpha$ -LA [10].

$\alpha$ -LA is a 123 residue  $\text{Ca}^{2+}$  binding protein found in mammalian milk which plays an active role in the synthesis of lactose [11,12]. The structure of  $\alpha$ -LA consists of two subdomains: an  $\alpha$ -helical domain ( $\alpha$ -domain) and a  $\beta$ -sheet domain ( $\beta$ -domain) [13–16] (Fig. 1) and is homologous to the C-type lysozymes [17,18]. In the molten globule state, the  $\alpha$ -domain contains significant helical structure, while the  $\beta$ -domain is largely unstructured [19–21]. The  $\alpha$ -domain consists of four  $\alpha$ -helices: the A-helix (residues 5–11), the B-helix (residues 23–34), the C-helix (residues 86–99) and the D-helix (residues 105–109), as well as a  $3_{10}$ -helix from residues 115 to 119. The A, B, D and  $3_{10}$ -helices are believed to be formed in the molten globule state while the C-helix is thought to be largely unfolded [22–24].  $\alpha$ -LA contains four disulfides, two of which are located in the  $\alpha$ -domain, one involving cysteine Cys<sup>28</sup> and Cys<sup>111</sup> and the other involving Cys<sup>6</sup> and Cys<sup>120</sup>. One of the remaining disulfides is found in the  $\beta$ -subdomain (Cys<sup>61</sup>-Cys<sup>77</sup>) and the other links the subdomains (Cys<sup>73</sup>-Cys<sup>91</sup>). The Cys<sup>28</sup>-Cys<sup>111</sup> disulfide has been shown to play an important role in stabilizing the molten globule state and mutants of  $\alpha$ -LA which contain only the Cys<sup>28</sup>-Cys<sup>111</sup> disulfide bond can still form a molten globule state [25].

The structure of the  $\alpha$ -LA molten globule state is not known, nor are the interactions which stabilize this state understood in detail. One particularly interesting question involves the balance between interactions involving residues which are close in primary sequence and interactions which involve residues which are further apart in the primary sequence. It is also of considerable interest to examine the potential for stabilizing interactions involving residues brought into close proximity by the two disulfide linkages in the structured  $\alpha$ -domain of the  $\alpha$ -LA molten globule. We have previously used synthetic peptides to examine the formation of structure near the Cys<sup>28</sup>-Cys<sup>111</sup> disulfide linkage [26]. Cys<sup>28</sup> is located in the B-helix and Cys<sup>111</sup> is found at the end of the D-helix. Both of these elements of secondary

structure are formed in the molten globule state [22]. Studies with synthetic peptides have shown that the B and C-helices are largely unstructured in isolation while the D-helix has a propensity to form a non-random structure in isolation [24,27–29]. Crosslinking peptides corresponding to the B and D-helices by the Cys<sup>28</sup>-Cys<sup>111</sup> disulfide bond resulted in a dramatic increase in structure [26]. An important conclusion resulting from that work was that the propensity for mutually stabilizing local interactions between regions of the peptide chain near the disulfide correlated with the key role played by the Cys<sup>28</sup>-Cys<sup>111</sup> disulfide in stabilizing the molten globule state.

In this work, we extend our studies to examine the role played by local interactions in the vicinity of the native Cys<sup>6</sup> to Cys<sup>120</sup> disulfide bond. Cys<sup>6</sup> is located within the A-helix while Cys<sup>120</sup> is in the C-terminal  $3_{10}$ -helix. Both of these elements of secondary structure are believed to be formed in the molten globule state of  $\alpha$ -LA and both provide important contributions to the stability of the molten globule state [30]. We examine the consequences of crosslinking the peptides derived from the N- and C-terminus by the native Cys<sup>6</sup>-Cys<sup>120</sup> disulfide bond. The results are compared to previous studies of peptides derived from regions near the Cys<sup>28</sup>-Cys<sup>111</sup> disulfide bond and provide insight into the role that local interactions involving residues near the disulfide bond play in the formation of the molten globule state. The Cys<sup>6</sup>-Cys<sup>120</sup> disulfide bond has been shown to be geometrically strained in the native structure [14] and hyperreactive [31,32], however, Kuwajima and coworkers have shown that the Cys<sup>6</sup>-Cys<sup>120</sup> disulfide bond does play a role in stabilizing the native and molten globule states [33]. Recent studies have also shown that point mutations at residues 8, 12 and 118, which are all located near this disulfide bond, perturb the stability of the molten globule state [34,35].

In this work, we also investigate the ability of the isolated peptides to fold. The N-terminal peptide contains the region corresponding to the A-helix and is particularly interesting since one of the most successful helix-predicting algorithms, AGADIR [36], suggests that there should be some propensity to populate helical structure in this region. In contrast, AGADIR predicts that the B and C-helices have very little propensity to fold in isolation. Recent

molecular dynamics simulations have also suggested that the A-helix is formed in the molten globule state while H/D exchange measurements show that the A-helix is moderately protected in the molten globule [37,38]. The C-terminal peptide consists of residues 112–123 and includes the C-terminal  $3_{10}$ -helix. AGADIR also predicts that the C-terminal region of the protein has some tendency to form a helical structure in isolation. Previous studies have examined peptides corresponding to the isolated B, C and D-helices [24,26,29,39]. Our study thus completes the analysis of peptides corresponding to isolated elements of secondary structure derived from the critical  $\alpha$ -domain of  $\alpha$ -LA.

Our study has implications for the interpretation of recent kinetic experiments which have examined the effect of reducing the Cys<sup>6</sup>-Cys<sup>120</sup> disulfide bond on folding and unfolding rates. Detailed interpretation of those experiments is aided by knowledge of the interactions which are present in the unfolded state under conditions which are relevant for folding. Unfortunately, the unfolded state cannot be studied directly under native conditions. Our 30 residue crosslinked peptide provides a good model of local interactions which could form in the vicinity of the Cys<sup>6</sup>-Cys<sup>120</sup> disulfide linkage.

## 2. Materials and methods

### 2.1. Peptide synthesis and purification

Peptides were synthesized on a 0.20 mmol scale on a Millipore 9050<sup>+</sup> automated peptide synthesizer using standard 9-fluorenylmethyloxycarbonyl (Fmoc) chemistry protocols. Use of a resin with a 5-(4'-Fmoc-aminomethyl-3',5'-dimethoxyphenoxy) valeric acid linker afforded C-terminal amidated peptides. Amino acid activation was carried out using 2-(1H-benzotriazol-1-yl)-1,1,3,3-tetramethyluronium tetrafluoroborate. The first residue to be attached to the resin, all  $\beta$ -branched amino acids and all residues directly following a  $\beta$ -branched residue were double coupled. A capping step consisting of a wash with a solution of 5% acetic anhydride, 5% pyridine, and 90% *N,N*-dimethylformamide (DMF) was used. The peptides were cleaved from the resin using a solution of 91% trifluoroacetic acid, 3% anisole, 3% thioani-

sole and 3% ethanedithiol. The crude peptides were purified by reverse phase high pressure liquid chromatography (HPLC) using a C-18 preparative column (Vydac). A two buffer system was utilized with hydrochloric acid (HCl) as the counterion. Buffer A consisted of H<sub>2</sub>O and 0.045% HCl (v/v). Buffer B consisted of 90% CH<sub>3</sub>CN and 10% H<sub>2</sub>O and 0.045% HCl (v/v). All peptides were analyzed at the CASM facility at the State University of New York at Stony Brook by a Bruker ProteinTOF matrix-assisted laser desorption ionization (MALDI) time of flight mass spectrometer (TOF-MS) using 3,5-dimethoxy-4-hydroxy-cinnamic acid (SA) as the matrix (Aldrich). The instrument was calibrated with several standards (SA (225.0), angiotensin (1047.0), substance P (1348.6), adrenocorticotrophic hormone (18–34) (2466.7) and bovine insulin (5734.5 for the singly charged species and 2867.7 for the doubly charged species)). All spectra were obtained in positive ion and reflectron mode. The expected molecular weight of  $\alpha$ -LA (1–13) is 1530, the observed molecular weight is 1531.7. The expected molecular weight of  $\alpha$ -LA (1–18) is 2129, the observed molecular weight is 2131.0. The expected molecular weight of  $\alpha$ -LA (112–123) is 1519, the observed molecular weight is 1519.5.

### 2.2. Formation of the native disulfide bond

Peptides were dissolved in either 6 M guanidine hydrochloride, 0.2 M Tris(hydroxymethyl)aminomethane (Tris), pH 8.5, or 0.2 M Tris, pH 8.5. The reaction was followed by HPLC using the same conditions utilized for purification of the peptides. MALDI TOF-MS was used to confirm the identity of the individual HPLC peaks.

### 2.3. Circular dichroism (CD)

CD measurements were made using an Aviv model 62DS instrument. Samples were prepared in a buffer of 2 mM borate, citrate and phosphate, 10 mM NaCl at pH 2.7 and 25°C. Peptide concentrations were determined by absorbance measurements at 280 nm using extinction coefficients calculated using the method of Pace and coworkers [40]. pH dependent studies were conducted by titrating a sample of peptide in a buffer of 2 mM borate, citrate and phos-

phate, 10 mM NaCl at 25°C with concentrated HCl and NaOH. The measured mean residue ellipticity at 222 nm was converted to the apparent fraction helix using the equations of Rohl and Baldwin [41].

#### 2.4. Sedimentation equilibrium

Solutions of the  $\alpha$ -LA (1–18) peptide and the 1–18/112–123 pair were dialyzed against a buffer containing 2 mM borate, citrate and phosphate, at either 10 mM NaCl or 100 mM NaCl at pH 2.7. Experiments were performed at 25°C with a Beckman XL-A analytical ultracentrifuge, using rotor speeds of 30 000, 40 000 and 50 000 rpm. Experiments were carried out using 12 mm pathlength, six-channel, charcoal-filled, Epon cells with quartz windows. Partial specific volumes were calculated from the weighted average of the partial specific volumes of the individual amino acids [42]. The data were fit globally with both a single-species and a multi-state model with the molecular mass treated as a fitting parameter. The HID program from the Analytical Ultracentrifugation Facility at the University of Connecticut was used for the fitting analysis.

#### 2.5. Fluorescence experiments

Fluorescence measurements were performed on an ISA Fluorolog spectrometer FL3-21. The concentration of 1-anilinonaphthalene-8-sulfonate (ANS) was determined using a value of  $8000 \text{ cm}^{-1} \text{ M}^{-1}$  as the molar absorption coefficient at 372 nm in methanol (provided by Molecular Probes). ANS fluorescence was excited at 370 nm and emission spectra were recorded over the range of 380–700 nm. Tryptophan fluorescence was excited at 280 nm and emission spectra were recorded from 285 to 450 nm.

#### 2.6. Nuclear magnetic resonance (NMR) spectroscopy

$^1\text{H}$  NMR experiments were carried out on Varian Unity INOVA 500 and 600 MHz spectrometers. Samples were prepared in 90%  $\text{H}_2\text{O}/10\%$   $\text{D}_2\text{O}$  and spectra were internally referenced to TSP at 0.0 ppm. 8K data points were collected in  $t_2$  for the DQF-COSY [43], while 2K data points were collected in  $t_2$  for TOCSY [44,45], NOESY [46] and ROESY [47]

experiments. A mixing time of 80 ms was used for the TOCSY experiment, while a mixing time of 300 ms was used for the NOESY (performed on  $\alpha$ -LA (1–18)) and ROESY (performed on  $\alpha$ -LA (112–123)) experiments. NMR data were processed using Felix95 (Biosym). The data sets were multiplied by a 90°-shifted sinebell window function and zero-filled once. Assignments were made using standard methods [48].  $^3J_{\text{HN}\alpha}$  coupling constants were determined from absorptive and dispersive peak separations in the DQF-COSY spectrum [49]. Chemical shift indices [50] were calculated using the random coil chemical shifts at 25°C from Wüthrich [48].

### 3. Results

The structure of human  $\alpha$ -LA is shown in Fig. 1. The region of the protein corresponding to the peptides studied in this work is indicated by black shading. The primary sequence of the peptides is included in Fig. 1. A peptide corresponding to residues 112–123 of  $\alpha$ -LA, denoted  $\alpha$ -LA (112–123), was prepared in order to test for the formation of locally stabilized structure in this region of the protein. This peptide contains the C-terminal 12 residues of  $\alpha$ -LA and includes the C-terminal  $3_{10}$ -helix. In addition, two peptides were prepared which encompass the A-helix. The first corresponds to residues 1–13 with Cys<sup>6</sup> replaced with an alanine, while the second corresponds to residues 1–18 and contains the native Cys<sup>6</sup>. This sequence includes the turn after the A-helix (residues 14–18). This peptide was prepared to help to elucidate the potential role of these residues in stabilizing the A-helix. The two peptides are denoted  $\alpha$ -LA (1–13) and  $\alpha$ -LA (1–18). A fourth peptide was prepared in which the 1–18 and 112–123 fragments were cross-linked via the native 6–120 disulfide bond and is denoted  $\alpha$ -LA (1–18/112–123).

In the remainder of this section, we first describe the results of CD and NMR studies of the conformational tendencies of  $\alpha$ -LA (112–123) in aqueous solution. We then discuss the results of a similar analysis of both the  $\alpha$ -LA (1–13) and  $\alpha$ -LA (1–18) peptides. We conclude by describing the effects on the structure which results from crosslinking  $\alpha$ -LA (1–18) and  $\alpha$ -LA (112–123) via the native Cys<sup>6</sup>-Cys<sup>120</sup> disulfide bond. This 30 residue fragment pro-

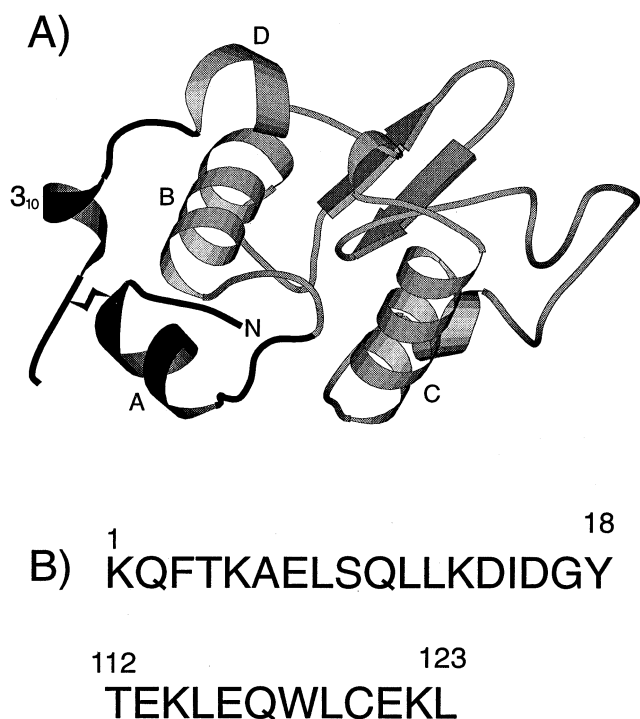


Fig. 1. (A) A MOLSCRIPT [54] diagram of human  $\alpha$ -LA. Residues 1–18 and 112–123 are shaded in black. Only the 6–120 disulfide bond is shown. The N-terminus is indicated as are the A, B, C, D and  $3_{10}$ -helices. (B) Sequences of the peptides studied in this work.

vides an excellent model system with which to probe for any potentially stabilizing interactions involving residues in the immediate vicinity of the disulfide bond [26]. This is a particularly interesting issue given our recent results on peptides derived from the region near the Cys<sup>28</sup>-Cys<sup>111</sup> disulfide bond. In that case, formation of the native disulfide bond led to a substantial increase in structure [26].

### 3.1. Conformational analysis of $\alpha$ -LA (112–123) in aqueous solution

The peptide corresponding to the C-terminal 12 residues of human  $\alpha$ -LA is largely unstructured as judged by CD, Fig. 2. The CD signal at 222 nm is independent of the concentration over the measured range of 10  $\mu$ M to 1 mM (data not shown). The value of  $\theta_{222}$  is  $-1700 \text{ deg cm}^2 \text{ dmol}^{-1}$  at pH 2.8, which corresponds to only 4% helix. There is only a modest change in  $\theta_{222}$  with pH. The values vary from  $-2000 \text{ deg cm}^2 \text{ dmol}^{-1}$  at pH 2.2 to  $-700 \text{ deg cm}^2 \text{ dmol}^{-1}$

at pH 9.0 (Fig. 3). No significant change in the helical content is detected at a low temperature. In 8 M urea, the value of  $\theta_{222}$  is  $+300 \text{ deg cm}^2 \text{ dmol}^{-1}$ , which indicates a lack of structure. The loss of the negative intensity at  $\theta_{222}$  upon the addition of urea demonstrates that the CD signal observed in H<sub>2</sub>O is due to a small amount of structure and is not caused by an anomalous random coil CD spectrum. The fraction helix can be calculated using the value of  $\theta_{222}$  in 8 M urea to represent the ellipticity of the coil state. The calculated value is 6% helix, which is in good agreement with the value calculated using the Rohl and Baldwin random coil values.

The <sup>1</sup>H spectrum of  $\alpha$ -LA (112–123) could be assigned using standard methods. Spin system assignments were accomplished using TOCSY and DQF-COSY spectra and a ROESY experiment was used to obtain sequential assignments. The NMR experiments are fully consistent with the CD studies and provide no evidence of any significant helical structure. The deviation of the  $\alpha$ -proton chemical shifts from random coil values is less than 0.2 ppm. The values of the <sup>3</sup>J<sub>HNC $\alpha$  coupling constants range from 5.7 to 7.2 Hz and are suggestive of conformational averaging. A complete set of sequential  $\alpha$  to amide ROEs was observed. Only two NH to NH (*i*,*i*+1) ROEs were observed and no  $\alpha$  to  $\beta$  or  $\alpha$  to NH (*i*,*i*+3) ROEs were observed. This pattern of ROEs is consistent with very little tendency to adopt a hel-</sub>

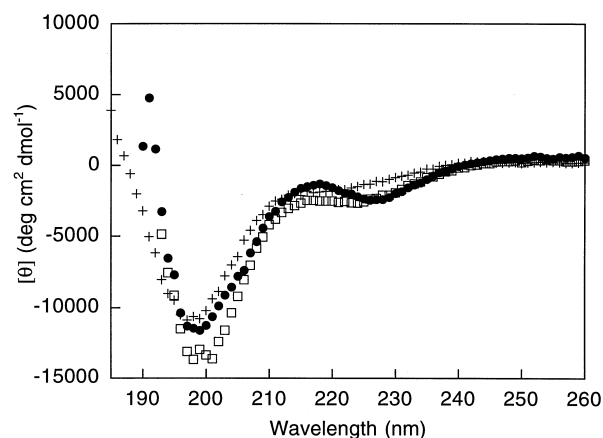


Fig. 2. CD spectra of  $\alpha$ -LA (1–13),  $\alpha$ -LA (1–18) and  $\alpha$ -LA (112–123) in 2 mM borate, citrate and phosphate, 10 mM NaCl, pH 2.7 at 25°C. Filled circles (●)  $\alpha$ -LA (1–13), open squares (□)  $\alpha$ -LA (1–18) and crosses (+)  $\alpha$ -LA (112–123).

ical structure. There are, however, a few sidechain to sidechain ROEs which are indicative of a non-random structure. A set of weak to moderate ROEs between the 7H and 4H sidechain protons of Trp<sup>118</sup> and the  $\delta\text{CH}_2$  and  $\epsilon\text{CH}_2$  sidechain protons of Lys<sup>114</sup> were observed. Additional ROEs were observed between the Trp<sup>118</sup> sidechain and the methyl groups of one or more leucines. Unfortunately, due to spectral overlap, it was not possible to resolve the methyl groups of Leu<sup>115</sup>, Leu<sup>119</sup> and Leu<sup>123</sup>. Studies with a shorter peptide which lacks Leu<sup>123</sup> show extensive contacts between Trp<sup>118</sup> and Leu<sup>119</sup> as well as several contacts between Trp<sup>118</sup> and Leu<sup>115</sup> [51].

### 3.2. $\alpha$ -LA (1–13) and $\alpha$ -LA (1–18) have a modest tendency to adopt a non-random structure

$\alpha$ -LA (1–13) appears to have only a modest tendency to populate helical structure. The value of  $\theta_{222}$  at 25°C, pH 2.7, is  $-2000 \text{ deg cm}^2 \text{ dmol}^{-1}$  (Fig. 2), which corresponds to approximately 5% helix using the method of Rohl and Baldwin. Although the values of  $\theta_{222}$  are similar, the shape of the spectrum is clearly different from that of  $\alpha$ -LA (112–123). The structure is abolished in 8 M urea ( $\theta_{222} = +200 \text{ deg cm}^2 \text{ dmol}^{-1}$ ). The fraction helix calculated using  $\theta_{222} = +200 \text{ deg cm}^2 \text{ dmol}^{-1}$  for the coil state is 7% helix. The value of  $\theta_{222}$  is somewhat pH dependent (Fig. 3), with a small increase in structure going from

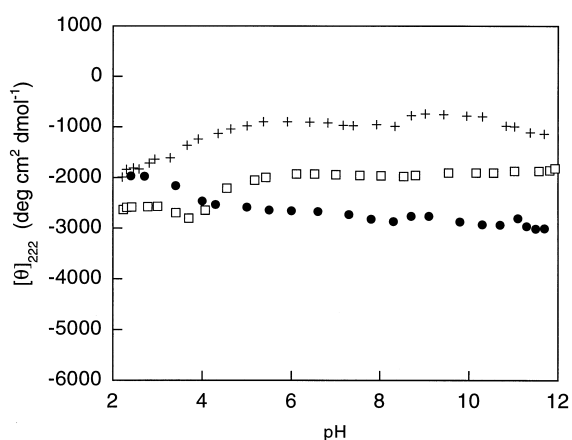


Fig. 3. pH dependence of the value of  $\theta_{222}$  for the individual peptides. Filled circles (●)  $\alpha$ -LA (1–13), open squares (□)  $\alpha$ -LA (1–18) and crosses (+)  $\alpha$ -LA (112–123). Measurements were made in 2 mM borate, citrate and phosphate, 10 mM NaCl, at 25°C.

pH 2.7 to 5.0. The value of  $\theta_{222}$  is maximum at pH 11.7, reaching a value of  $\theta_{222} = -3000 \text{ deg cm}^2 \text{ dmol}^{-1}$ , which corresponds to approximately 10% helix and is minimum at pH 2.4, where  $\theta_{222} = -1900 \text{ deg cm}^2 \text{ dmol}^{-1}$ . No significant increase in helicity is observed at lower temperatures.

The addition of residues 14–18 slightly increases the amount of helical structure at low pH as judged by the value of  $\theta_{222}$ , although the overall helical content of the peptide is still relatively small. The value of  $\theta_{222}$  observed for  $\alpha$ -LA (1–18) is  $-3000 \text{ deg cm}^2 \text{ dmol}^{-1}$  (Fig. 2), which corresponds to approximately 8% helix using the Rohl and Baldwin value for  $\theta_{222}$  of the coil state. The structure is abolished in 8 M urea ( $\theta_{222}$  is weakly positive,  $+400 \text{ deg cm}^2 \text{ dmol}^{-1}$ ). The fraction helix calculated using the  $\theta_{222} = +400 \text{ deg cm}^2 \text{ dmol}^{-1}$  for the coil state is 10%. The pH profile is different than that of  $\alpha$ -LA (1–13), but again, the changes are relatively modest.  $\theta_{222}$  ranges from  $-2800 \text{ deg cm}^2 \text{ dmol}^{-1}$  at pH 3.6 to  $-1820 \text{ deg cm}^2 \text{ dmol}^{-1}$  at pH 11.9. A decrease in structure above pH 4 is observed, perhaps due to unfavorable electrostatic interactions that may result when the sidechains of the two additional aspartic acids near the C-terminus are deprotonated. Above pH 4,  $\alpha$ -LA (1–13) appears slightly more structured than  $\alpha$ -LA (1–18), as judged by the value of  $\theta_{222}$ . Analytical ultracentrifugation demonstrates that the peptide is monomeric at concentrations below 50  $\mu\text{M}$ , but that by 1 mM, approximately 20% of the peptide is aggregated. Because the peptide shows some aggregation at the higher concentration, detailed quantitative analysis of the NMR data is not possible. The NMR spectrum is, however, independent of the concentration over the measured range of 400  $\mu\text{M}$  to 4 mM and the peaks are sharp.  $\theta_{222}$  is also independent of the concentration over the measured range of 20  $\mu\text{M}$  to 1 mM. The NMR resonances could be assigned using standard methods. Only a single set of resonances is observed in the NMR spectrum, indicating that the monomeric form is in fast exchange with the small population of associated species. The observed chemical shifts are a population-weighted average of the shifts due to each association state. Since the monomeric state is the dominant species, the observed chemical shifts are likely to largely reflect the monomeric state. Interpretation of individual chemical shift values is problematic, but comparison

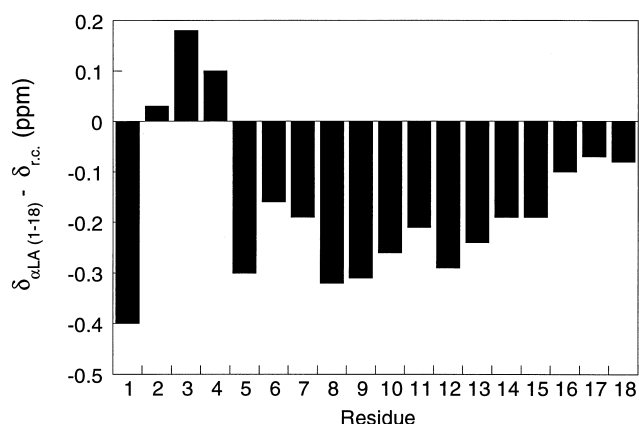


Fig. 4. Deviation of the  $\alpha$ -proton chemical shifts of  $\alpha$ -LA (1–18) from random coil values. Measurements were made at pH 2.7, 25°C at a peptide concentration of 4 mM.

of the shifts of different residues should be useful. Although we are cautious not to place undue emphasis on the NMR data, it is interesting to note that the pattern of  $\alpha$ -proton shifts is suggestive of a slight propensity to populate the helical structure after Thr<sup>4</sup>, suggesting that Thr<sup>4</sup> may act as a capping residue (Fig. 4). The  $\alpha$ -proton shifts of residues 2–4 and 16–18 are all within 0.2 ppm downfield of random coil values. The first residue is strongly perturbed by the charged N-terminus and thus, the deviation of this residue from random coil values does not reflect secondary structure. In contrast, the  $\alpha$ -proton resonances of residues 5–15 are all shifted upfield of the random coil values by 0.2–0.3 ppm. In the crystal structure of intact  $\alpha$ -LA, the A-helix begins at residue 5 and the Thr<sup>4</sup> hydroxyl group acts as a capping residue by hydrogen bonding to the amide proton of Cys<sup>6</sup>. The measured chemical shifts indicate that  $\alpha$ -LA (1–18) has a propensity for a native-like helical structure in isolation that may be partially facilitated by the native capping interaction of Thr<sup>4</sup>. The helical propensity observed for residues 5–15 of  $\alpha$ -LA (1–18) extends three residues beyond the native A-helix which terminates at Leu<sup>12</sup>.

### 3.3. The structural consequences of crosslinking $\alpha$ -LA (1–18) and $\alpha$ -LA (112–123) by the native Cys<sup>6</sup>-Cys<sup>120</sup> disulfide bond

When  $\alpha$ -LA (1–18) and  $\alpha$ -LA (112–123) are cross-linked via Cys<sup>6</sup> and Cys<sup>120</sup> ( $\alpha$ -LA (1–18/112–123)),

only a small increase in helicity is observed. The value of  $\theta_{222}$  measured at pH 2.8, 25°C is  $-3300 \text{ deg cm}^2 \text{ dmol}^{-1}$ , which corresponds to 9% helix as determined by using the Rohl and Baldwin equations (Fig. 5A). This represents only a small increase in helicity relative to that expected for the sum of the reduced peptides.  $\theta_{222}$  would equal  $-2200 \text{ deg cm}^2 \text{ dmol}^{-1}$  if there was no increase in structure upon

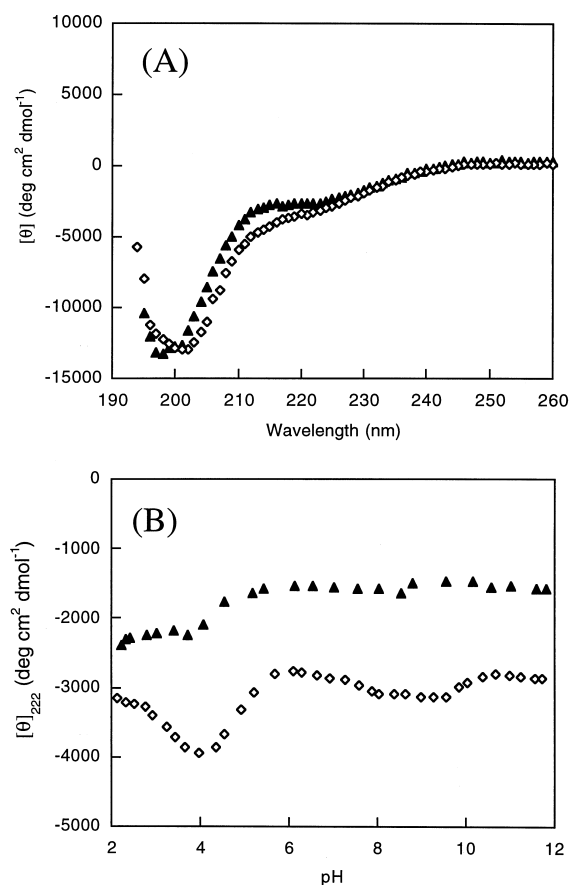


Fig. 5. (A) Comparison of the CD spectrum of  $\alpha$ -LA (1–18/112–123) with the CD spectrum corresponding to the summation of the spectra of  $\alpha$ -LA (1–18) and  $\alpha$ -LA (112–123). Filled triangles (▲) represent the value expected from the normalized summation of 1–18 and 112–123, while the open diamonds (◇) correspond to the oxidized construct  $\alpha$ -LA (1–18/112–123). Measurements were made in 2 mM borate, citrate and phosphate, 10 mM NaCl, pH 2.7, at 25°C. (B) pH dependence of the value of  $\theta_{222}$  for the  $\alpha$ -LA (1–18/112–123) construct and the normalized summation of  $\theta_{222}$   $\alpha$ -LA (1–18) and  $\alpha$ -LA (112–123). Filled triangles (▲) are the summation of  $\alpha$ -LA (1–18) and  $\alpha$ -LA (112–123), while the open diamonds (◇) are the oxidized construct  $\alpha$ -LA (1–18/112–123). Measurements were made in 2 mM borate, citrate and phosphate, 10 mM NaCl at 25°C.

formation of the crosslink. If the construct was as helical as the same region of the intact protein, a value of  $\theta_{222} = -15868 \text{ deg cm}^2 \text{ dmol}^{-1}$  would be observed. This demonstrates that formation of the disulfide does not induce any significant increase in structure. This is in sharp contrast to our previous studies of peptide fragments corresponding to the sequence of the protein chain near the Cys<sup>28</sup>-Cys<sup>111</sup> disulfide bond. In that case, a significant enhancement in structure was observed upon formation of the disulfide.

Our results are not an artifact of the pH chosen for the experiments. When the pH profiles of  $\alpha$ -LA (1–18) and  $\alpha$ -LA (112–123) are summed and normalized and compared with that of  $\alpha$ -LA (1–18/112–123), only small differences are observed. This is an important control since it is known that  $\alpha$ -LA can form a molten globule state at both acidic and neutral pH. The average difference in  $\theta_{222}$  between the oxidized construct and the sum of the value of  $\theta_{222}$  for the individual peptides over the entire pH range is  $-1340 \text{ deg cm}^2 \text{ dmol}^{-1}$  and the maximum difference between the two is  $-1700 \text{ deg cm}^2 \text{ dmol}^{-1}$  at pH 3.7. This represents a 27% difference. However, the actual value of  $\theta_{222} = -3800 \text{ deg cm}^2 \text{ dmol}^{-1}$  represents only a modest amount of structure. The complete pH profile is displayed in Fig. 5B. The structure of the crosslinked peptide is abolished upon the addition of chemical denaturants. The value of  $\theta_{222}$  decreases by two thirds in only 0.5 M urea and becomes weakly positive in 8 M urea ( $\theta_{222} = +300 \text{ deg cm}^2 \text{ dmol}^{-1}$ ). The fraction helix calculated using a value of  $\theta_{222} = +300 \text{ deg cm}^2 \text{ dmol}^{-1}$  for the coil state is 10%. The construct is monomeric below 20  $\mu\text{M}$  in aqueous solutions as judged by analytical ultracentrifugation and concentration dependent CD measurements. Above 50  $\mu\text{M}$ , self-association was detected.

The fluorescence emission spectrum of the construct is consistent with exposure of the sole tryptophan residue to solvent ( $\lambda_{\text{max}} = 355 \text{ nm}$ ). The near UV-CD spectrum of  $\alpha$ -LA (1–18/112–123) contains very weak bands (data not shown) and is consistent with a lack of significant structure. In order to test for the formation of loosely packed hydrophobic surfaces, a fluorescence-monitored ANS titration was performed. No significant increase in the ANS fluorescence intensity or shift in the emission maximum

was observed even with a 5-fold excess of peptide, indicating that the construct does not bind ANS. Again, this is in contrast to previous studies of peptides derived from the region of the Cys<sup>28</sup>-Cys<sup>111</sup> disulfide bond. In that case, peptides corresponding to the crosslinked B and D-helices bound ANS [26].

#### 4. Discussion

Our results demonstrate that the A-helix of  $\alpha$ -LA has a slight tendency to adopt a helical structure in isolation. Although the helical content is low, the peptide is more structured than a peptide derived from the isolated B-helix (D.F.M., S.J.D. and D.P.R., unpublished results). The C-terminal 12 residue peptide, which encompasses the  $3_{10}$ -helix, appears to be even less helical in aqueous medium. The formation of the native Cys<sup>6</sup>-Cys<sup>120</sup> disulfide bond does not promote a significant amount of structure at any pH. This is an interesting result since it indicates that local interactions between residues near the site of the crosslink are not sufficient to promote structure formation.

The results presented here offer a striking contrast to our previous work on peptides involving the Cys<sup>28</sup>-Cys<sup>111</sup> disulfide linkage. In that case, formation of the disulfide bond resulted in a significant increase in structure. Thus, there appears to be a correlation between the importance of the individual disulfides to the stability of the  $\alpha$ -LA molten globule and the propensity for mutually stabilizing interactions between the regions of the protein chain brought into proximity by formation of the crosslink [20]. In this sense, interactions involving residues localized in the vicinity of the disulfide appear to contribute significantly to the enhancement of structure upon formation of the Cys<sup>28</sup>-Cys<sup>111</sup> linkage, but not for the Cys<sup>6</sup>-Cys<sup>120</sup> disulfide bond.

$\alpha$ -LA forms a molten globule state at low pH when the Cys<sup>6</sup>-Cys<sup>120</sup> disulfide bond is reduced. The molten globule which is formed is structurally similar, though less stable, than the molten globule state of intact  $\alpha$ -LA [33]. The change in stability likely includes a contribution due to increased conformational entropy in the unfolded state. The conformational entropy of the molten globule state will also be larger, but the effect should be smaller be-



cause the molten globule likely brings residues 6 and 120 into closer proximity. There may also be a contribution from stabilizing interactions involving residues near the Cys<sup>6</sup>-Cys<sup>120</sup> disulfide bond which could be lost or diminished when the disulfide is reduced. The results of this study indicate that these interactions, if they are indeed present, cannot simply be due to local effects involving just the residues in the immediate proximity of the disulfide bond.

In other work, we have used large peptide models to define the structured core of the  $\alpha$ -LA molten globule. The core structure includes the region of the protein which encompasses the A-helix and the C-terminal <sub>310</sub>-helix [30]. Those experiments demonstrated that the A-helix region and <sub>310</sub>-helix region are critical for the formation of a stable molten globule. The work described in this study has shown that the structure in these regions is not significantly stabilized by purely local interactions or by interactions involving residues near the disulfide bond. Interactions involving the remainder of the chain are clearly required to lead to the structure in the region of the Cys<sup>6</sup>-Cys<sup>120</sup> disulfide bond. Again, this is in contrast to the region near the Cys<sup>28</sup>-Cys<sup>111</sup> disulfide bond. Our work also has relevance for the characterization of the unfolded state of  $\alpha$ -LA since it suggests that there is unlikely to be any notable tendency to populate the locally stabilized native structure in the vicinity of the Cys<sup>6</sup>-Cys<sup>120</sup> disulfide bond in the unfolded state.

This study also aids in the interpretation of recent experimental studies of the kinetics of  $\alpha$ -LA folding. Reduction of the Cys<sup>6</sup>-Cys<sup>120</sup> disulfide bond of  $\alpha$ -LA has been shown to result in an acceleration of the unfolding rate and to have only a very small effect upon the folding rate [52]. One interpretation of these results is that the structure involving residues near the Cys<sup>6</sup>-Cys<sup>120</sup> disulfide bond is not formed in the transition state for folding [52]. Alternatively, this region of the protein could be equally structured in both the transition state and in the denatured state and consolidation of the structure could take place after the rate limiting step. Examples of this sort of behavior, where an element of native-like structure is formed in the transition state but is not kinetically important for folding, have recently been observed in folding studies of the N-terminal domain of L9 [53]. In that case, the native structure corresponding to an

$\alpha$ -helix was pre-formed in the denatured state and was also structured in the transition state. In order to formally exclude the possibility that interactions near the 6-120 disulfide bond are formed in the unfolded state, one would need to study the conformation of the denatured state under conditions which are relevant for folding, i.e. under conditions in which the native state is stable. This is obviously impossible to do in a direct fashion since the unfolded state is only transiently populated under native conditions. Our crosslinked peptide provides a good model of local structure in the region of the 6-120 disulfide in the denatured state. The fact that no significant structure is observed strongly supports the first interpretation of the results of the kinetics experiments and argues against the second.

### Acknowledgements

This work was supported by NIH Grant GM54233 to D.P.R. D.P.R. is a Pew Scholar in the Biomedical Sciences. D.F.M. and S.J.D. were supported in part by GAANN Fellowships from the Department of Education. The analytical ultracentrifuge was purchased using funds from a grant to R.F. from the Zimmer Corporation.

### References

- [1] K. Kuwajima, The molten globule state as a clue for understanding the folding and cooperativity of globular-protein structure, *Proteins Struct. Funct. Genet.* 6 (1989) 87–103.
- [2] K. Kuwajima, The molten globule state of  $\alpha$ -lactalbumin, *FASEB J.* 10 (1996) 102–109.
- [3] O.B. Ptitsyn, Molten globule and protein folding, *Adv. Protein Chem.* 47 (1995) 83–222.
- [4] T.E. Creighton, How important is the molten globule for correct protein folding?, *Trends Biochem. Sci.* 22 (1997) 6–10.
- [5] D.A. Dolgikh, R.I. Gilmanishin, E.V. Brazhnikov, V.E. Bychkova, G.V. Semisotnov, S.Y. Venyaminov, O.B. Ptitsyn,  $\alpha$ -lactalbumin: Compact state with fluctuating tertiary structure?, *FEBS Lett.* 136 (1981) 311–315.
- [6] D.A. Dolgikh, L.V. Abaturon, I.A. Bolotina, E.V. Brazhnikov, V.E. Bychkova, V.N. Bushuev, R.I. Gilmanishin, Y.O. Levedev, G.V. Semisotnov, E.I. Tiktopulo, O.B. Ptitsyn, Compact state of a protein molecule with pronounced small-scale mobility: Bovine  $\alpha$ -lactalbumin, *Eur. Biophys. J.* 13 (1985) 109–121.

- [7] K. Kuwajima, K. Nitta, M. Yoneyama, S. Sugai, Three-state denaturation of  $\alpha$ -lactalbumin by guanidine hydrochloride, *J. Mol. Biol.* 106 (1976) 359–373.
- [8] K. Kuwajima, M. Mitani, S. Sugai, Characterization of the critical state in protein folding: Effects of guanidine hydrochloride and specific  $\text{Ca}^{2+}$  binding of the folding kinetics of  $\alpha$ -lactalbumin, *J. Mol. Biol.* 206 (1989) 547–561.
- [9] D.T. Haynie, E. Friere, Structural energetics of the molten globule state, *Proteins Struct. Funct. Genet.* 16 (1993) 115–140.
- [10] M. Ikeguchi, K. Kuwajima, M. Mitani, S. Sugai, Evidence for identity between the equilibrium unfolding intermediate and a transient folding intermediate A comparative study of the folding reactions of  $\alpha$ -lactalbumin and lysozyme, *Biochemistry* 25 (1986) 6965–6972.
- [11] H. Babad, W.Z. Hassid, A soluble lactose-synthesizing enzyme from bovine milk, *J. Biol. Chem.* 239 (1964) 946–948.
- [12] Y. Hiraoka, T. Segawa, K. Kuwajima, S. Sugai, N. Murai,  $\alpha$ -lactalbumin: A calcium metalloprotein, *Biochem. Biophys. Res. Commun.* 95 (1980) 1098–1104.
- [13] K.R. Acharya, D.I. Stuart, N.P.C. Walker, M. Lewis, D.C. Phillips, Refined structure of baboon  $\alpha$ -lactalbumin at 1.7 Å resolution, *J. Mol. Biol.* 208 (1989) 99–127.
- [14] K.R. Acharya, J. Ren, D.I. Stuart, D.C. Phillips, R.E. Fenna, Crystal structure of human  $\alpha$ -lactalbumin at 1.7 Å resolution, *J. Mol. Biol.* 221 (1991) 571–581.
- [15] K. Harata, M. Muraki, X-ray structural evidence for a local helix-loop transition in  $\alpha$ -lactalbumin, *J. Biol. Chem.* 267 (1992) 1419–1421.
- [16] A.C. Pike, K. Brew, K.R. Acharya, Crystal structures of guinea-pig, goat and bovine  $\alpha$ -lactalbumin highlight the enhanced conformational flexibility of regions that are significant for its action in lactose synthase, *Structure* 4 (1996) 691–703.
- [17] H.A. McKenzie, F.H. White Jr., Lysozyme and  $\alpha$ -lactalbumin: Structure, function, and interrelationships, *Adv. Protein Chem.* 41 (1991) 171–315.
- [18] P.K. Qasba, S.K. Saraya, Similarity of the nucleotide sequences of rat  $\alpha$ -lactalbumin and chicken lysozyme genes, *Nature* 308 (1984) 377–380.
- [19] B.A. Schulman, C. Redfield, Z.Y. Peng, C.M. Dobson, P.S. Kim, Different subdomains are most protected from hydrogen exchange in the molten globule and native states of human  $\alpha$ -lactalbumin, *J. Mol. Biol.* 253 (1995) 651–657.
- [20] L.C. Wu, Z.Y. Peng, P.S. Kim, Bipartite structure of the  $\alpha$ -lactalbumin molten globule, *Nat. Struct. Biol.* 2 (1995) 281–286.
- [21] J. Baum, C.M. Dobson, P.A. Evans, C. Hanley, Characterization of a partly folded protein by NMR methods studies on the molten globule state of guinea pig  $\alpha$ -lactalbumin, *Biochemistry* 28 (1989) 7–13.
- [22] B.A. Schulman, P.S. Kim, Proline scanning mutagenesis of a molten globule reveals non-cooperative formation of a protein's overall topology, *Nat. Struct. Biol.* 3 (1996) 682–687.
- [23] Z. Peng, P.S. Kim, A protein dissection study of a molten globule, *Biochemistry* 33 (1994) 2136–2141.
- [24] B.A. Kuhlman, J.A. Boice, W. Wu, R. Fairman, D.P. Raleigh, Calcium binding peptides from  $\alpha$ -lactalbumin Implications for protein folding and stability, *Biochemistry* 37 (1997) 4607–4613.
- [25] Z.Y. Peng, L.C. Wu, P.S. Kim, Local structural preferences in the  $\alpha$ -lactalbumin molten globule, *Biochemistry* 34 (1995) 3248–3252.
- [26] S.J. Demarest, R. Fairman, D.P. Raleigh, Peptide models of local and long-range interactions in the molten globule state of human  $\alpha$ -lactalbumin, *J. Mol. Biol.* 283 (1998) 279–291.
- [27] L.J. Smith, A.T. Alexandrescu, M. Pitkeathly, C.M. Dobson, Solution structure of a peptide fragment of human  $\alpha$ -lactalbumin in trifluoroethanol A model for local structure in the molten globule, *Structure* 2 (1994) 703–712.
- [28] A. Shimizu, M. Ikeguchi, T. Kobayashi, S. Sugai, A synthetic peptide study on the molten globule of  $\alpha$ -lactalbumin, *J. Biochem.* 119 (1996) 947–952.
- [29] A.T. Alexandrescu, P.A. Evans, M. Pitkeathly, J. Baum, C.M. Dobson, Structure and dynamics of the acid-denatured molten globule state of  $\alpha$ -lactalbumin A two-dimensional NMR study, *Biochemistry* 32 (1993) 1707–1718.
- [30] S.J. Demarest, J.A. Boice, R. Fairman, D.P. Raleigh, Defining the core structure of the  $\alpha$ -lactalbumin molten globule state, *J. Mol. Biol.* (1999) in press.
- [31] K. Kuwajima, M. Ikeguchi, T. Sugawara, Y. Hiraoka, S. Sugai, Kinetics of disulfide bond reduction in  $\alpha$ -lactalbumin by dithiothreitol and molecular basis of superreactivity of the Cys6-Cys120 disulfide bond, *Biochemistry* 29 (1990) 8240–8249.
- [32] Y. Shechter, A. Patchornik, Y. Burstein, Selective reduction of cystine I-VIII in  $\alpha$ -lactalbumin of bovine milk, *Biochemistry* 12 (1973) 3407–3413.
- [33] M. Ikeguchi, S. Sugai, M. Fujino, T. Sugawara, K. Kuwajima, Contribution of the 6-120 disulfide bond of  $\alpha$ -lactalbumin to the stabilities of its native and molten globule states, *Biochemistry* 31 (1992) 12695–12700.
- [34] J. Song, P. Bai, L. Luo, Z.Y. Peng, Contribution of individual residues to formation of the native-like tertiary topology in the  $\alpha$ -lactalbumin molten globule, *J. Mol. Biol.* 280 (1998) 167–174.
- [35] L.C. Wu, P.S. Kim, A specific hydrophobic core in the  $\alpha$ -lactalbumin molten globule, *J. Mol. Biol.* 280 (1998) 175–182.
- [36] V. Muñoz, L. Serrano, Development of the multiple sequence approximation within the AGADIR model of  $\alpha$ -helix formation: Comparison with Zimm-Bragg and Lifson-Roig formalisms, *Biopolymers* 41 (1997) 495–509.
- [37] L.J. Smith, C.M. Dobson, W.F. van Gunsteren, Sidechain conformational disorder in a molten globule: molecular dynamics simulations of the A-state of human  $\alpha$ -lactalbumin, *J. Mol. Biol.* 286 (1999) 1567–1580.
- [38] V. Forge, R.T. Wijesinha, J. Balbach, K. Brew, C.V. Robinson, C. Redfield, C.M. Dobson, Rapid collapse and slow structural reorganization during the refolding of bovine  $\alpha$ -lactalbumin, *J. Mol. Biol.* 288 (1999) 673–688.
- [39] S.J. Demarest, Y. Hua, D.P. Raleigh, Local interactions

- drive the formation of non-native structure in the denatured state of human  $\alpha$ -lactalbumin A high resolution structural characterization of a peptide model in aqueous solution, *Biochemistry* 38 (1999) 7380–7387.
- [40] C.N. Pace, F. Vajdos, L. Fee, G. Grimsley, T. Gray, How to measure and predict the molar absorption coefficient of a protein, *Protein Sci.* 4 (1995) 2411–2423.
- [41] C.A. Rohl, R.L. Baldwin, Comparison of N-H exchange and circular dichroism as techniques for measuring the parameters of helix-coil transition in peptides, *Biochemistry* 36 (1997) 8435–8442.
- [42] T.M. Laue, B.D. Shah, T.M. Rigdeway, S.L. Pelletier, in: S.E. Harding, A.J. Rowe, J.C. Horton (Eds.), *Analytical Ultracentrifugation in Biochemistry and Polymer Science*, The Royal Society of Chemistry, Cambridge, 1992, pp. 90–125.
- [43] U. Piantimi, O.W. Sorensen, R.R. Ernst, Multiple quantum filters for elucidating NMR coupling networks, *J. Am. Chem. Soc.* 104 (1982) 6800–6801.
- [44] L. Braunschweiler, R.R. Ernst, Coherence transfer by isotropic mixing: Application of proton correlation spectroscopy, *J. Magn. Reson.* 53 (1983) 521–528.
- [45] D.G. Davis, A. Bax, Assignment of complex H1-NMR spectra via two-dimensional homonuclear Hartmann-Hahn spectroscopy, *J. Am. Chem. Soc.* 107 (1985) 2820–2821.
- [46] A. Kumar, G. Wagner, R.R. Ernst, K. Wüthrich, Studies of J-connectivities and selective  $^1\text{H}$ - $^1\text{H}$  Overhauser effects in  $\text{H}_2\text{O}$  solutions of biological macromolecules by two-dimensional NMR experiments, *Biochem. Biophys. Res. Commun.* 96 (1980) 1156–1163.
- [47] A.A. Bothner-By, R.L. Stephens, J.-M. Lee, C.D. Warren, R.W. Jeanloz, Structural determination of a tetrasaccharide: Transient nuclear Overhauser effects in the rotating frame, *J. Am. Chem. Soc.* 106 (1984) 811–813.
- [48] K. Wüthrich, *NMR of Proteins and Nucleic Acids*, John Wiley and Sons, New York, 1986.
- [49] Y. Kim, J.H. Prestegard, Measurement of vicinal couplings from cross peaks in COSY spectra, *J. Magn. Reson.* 84 (1989) 9–13.
- [50] D.S. Wishart, B.D. Sykes, F.M. Richards, The chemical shift index A fast and simple method for the assignment of protein secondary structure through NMR spectroscopy, *Biochemistry* 31 (1992) 1647–1651.
- [51] S.J. Demarest, D.P. Raleigh, The solution structure of a peptide model of a region important for the folding of  $\alpha$ -lactalbumin provides evidence for the formation of non-native structure in the denatured state, *Proteins Struct. Funct. Genet.* (1999) in press.
- [52] I. Ikeguchi, M. Fujino, M. Kato, K. Kuwajima, S. Sugai, Transition state in the folding of alpha-lactalbumin probed by the 6-120 disulfide bond, *Protein Sci.* 7 (1998) 1564–1574.
- [53] D.L. Luisi, B. Kuhlman, K. Sideras, P.A. Evans, D.P. Raleigh, Effects of varying the local propensity to form secondary structure on the stability and folding kinetics of a rapid folding mixed  $\alpha/\beta$  protein: Characterization of a truncation mutant of the N-terminal domain of the ribosomal protein L9, *J. Mol. Biol.* 289 (1999) 167–174.
- [54] P.J. Kraulis, MOLSCRIPT: a program to produce both detailed and schematic plots of protein structures, *J. Appl. Crystallogr.* 24 (1991) 946–950.